

경화 시스템이 천연고무계 자기유변탄성체의 계면접착 및 기계적 특성에 미치는 영향

고천명*** · 나복균* · 김남윤* · 정경호*[†]

*수원대학교 신소재공학과

**Agricultural Product Processing Research Institute, Chinese Academy of Tropical Agriculture Science
(2017년 11월 6일 접수, 2018년 2월 21일 수정, 2018년 2월 22일 채택)

Interfacial Adhesion and Mechanical Properties of Magneto-rheological Elastomer Based on the Natural Rubber with Different Curing System

Tianming Gao***, Bokgyun Na*, Namyun Kim*, and Kyungho Chung*[†]

*Department of Polymer Engineering, The University of Suwon, Hwaseong-Si, Gyeonggi-Do 445743, Korea

**Agricultural Product Processing Research Institute, Chinese Academy of Tropical Agriculture Science, Zhanjiang 524001, China
(Received November 6, 2017; Revised February 21, 2018; Accepted February 22, 2018)

초록: 엘라스토머 가공에서 가황반응은 매우 중요한 공정이다. 천연고무(NR)를 사용한 자기유변탄성체(MRE)에 관한 연구들은 많이 수행되어 왔지만 엘라스토머 경화 시스템이 천연고무계 MRE의 계면접착 및 기계적 특성에 미치는 영향에 대해서는 연구가 거의 이루어지지 않았다. 본 연구에서는 경화제로 황과 디큐밀퍼옥사이드(DCP)를 사용하여 이들이 NR계 MRE의 특성에 미치는 영향을 조사하였다. MRE 매트릭스에 분산된 카보닐 철 입자(CIP)와 매트릭스의 계면 접착력은 주사전자현미경을 사용하여 분석하였다. 결과에 따르면 경화제로 황을 사용할 경우보다 DCP를 사용할 경우 MRE의 가교도가 높았다. 또한 CIP가 30 vol% 배합되었을 때 DCP 경화 시스템의 경우는 인장강도가 증가하였지만, 황 경화 시스템의 경우는 감소하였다. 개선된 DMA 장치를 사용하여 자기장이 인가된 상태에서 MRE의 자기유변 특성이 조사되었다.

Abstract: Vulcanization is an important procedure for elastomers processing. The effects of vulcanization system on the interfacial interaction and mechanical properties of magneto-rheological elastomers (MREs) based on natural rubber (NR) have not been researched, even though, there were many researches focusing on the natural rubber based MREs. In this work, sulfur and dicumyl peroxide (DCP) acted as curing agents preparing MREs based on NR. Scanning electron microscopy was used to characterize the interfacial adhesion of carbonyl iron particles (CIPs) in the matrix. Crosslink density provided evidence that the MREs with DCP system had higher crosslink density than that of MREs with sulfur system. The tensile strength of MREs with DCP system increased, while that of MREs with sulfur system decreased, when 30 vol% of CIPs filled into NR. Finally, the magneto-induced dynamic mechanical properties were tested using a modified dynamic thermo-mechanical analysis under magnetic fields.

Keywords: magneto-rheological elastomer, natural rubber, vulcanization system, mechanical properties, interfacial adhesion.

Introduction

Magneto-rheological elastomers (MREs) are functional materials due to the dynamic and rheological properties that can be stimulated by an external magnetic field.^{1,2} Therefore, MREs have been applied in a wide range, including adaptively

tuned vibration absorbers,^{3,4} suspension bushing,⁵ seismic protection,⁶ magneto-resistor sensors,^{7,8} noise barrier systems,⁹ and electric current active element.¹⁰ MREs are composed of magnetic particles, elastomers, and additives. Many types of elastomers have been applied for MREs fabrication, such as natural rubber,¹¹⁻¹⁶ silicone rubber,¹⁷ polyurethane,¹⁸ polychloroprene rubber,¹⁹ EPDM,²⁰ and cis-polybutadiene rubber (BR).²¹

Vulcanization is an important procedure in rubber processing. The rubber changes into elastic vulcanizate by vulcanization via

[†]To whom correspondence should be addressed.
khchung@suwon.ac.kr, ORCID[®] 0000-0001-9906-4634
©2018 The Polymer Society of Korea. All rights reserved.

chemical reactions. The fundamental aim of vulcanization is cross-linking of macromolecules, which results in a three-dimensional network.²² Sulfur and peroxide cure system are two main curing systems for rubber vulcanization technologies. Peroxide vulcanization is initiated by radical to form carbon-carbon crosslink structure, and homogeneous or uniform networks in the rubber matrix. Sulfur vulcanization is crosslinked by sulfur to form sulfur crosslink structure, including polysulfides, disulfides, mono-sulfides etc. and inhomogeneity of network structures existed in the rubber matrix.²³ Therefore, different cure system showed different tensile strength and strain-induced crystallization behavior.

Natural rubber (NR) is harvested from *Hevea brasiliensis*, and is widely used in various fields because of its superior elasticity, flexibility, and resilience.²⁴ Hence, NR could not be totally replaced by other types of rubber in industry due to the excellent comprehensive performance. The advantageous properties of NR and its suitability for preparing MREs have attracted great attention. Chen¹¹ discussed the effects of carbon black on mechanical performances in MREs based on NR. However, the maximum content of carbon black was 7%, and they did not mention about vulcanization system. Chung¹² found that peptizer decreased viscosity and molecular weight of NR matrix with sulfur vulcanization system, and resulted in efficient orientation of carbonyl iron particles (CIPs) and higher MR effect. Ge¹³ used rosin glycerin ester to enhance wettability and dispersibility of CIPs in the NR. It decreased zero-field modulus of MREs and increased magnetic-induced storage modulus and MR effect of MREs. As with Chen's work, they also did not mention about the additive. Choi's group^{14,15} fabricated the MREs using pure CIPs and surface modified CIPs. The results showed that storage modulus, loss modulus, and MR effect of MREs increased when the surface modified CIPs filled in the NR matrix. However, a curing agent was not used in the MREs matrix. Pickering¹⁶ modified the iron sand using bis-(3-triethoxysilylpropyl) tetrasulphane (TESPT), and prepared the MREs using surface modified iron sand based on NR with sulfur curing system. Overall, the previous studies of MREs based on NR have focused on improving interfacial compatibility and enhancing mechanical properties via surface modification of magnetic particles and plasticizer filled elastomers. To our knowledge there has not been any research focusing on the impact on the interface between CIPs and rubber molecules and the properties of curing agent system in the MREs based on NR.

The interfacial adhesion between inorganic particles and

elastomers molecules is a common problem in the composites of elastomers matrix. How to solve this question is the main research in this domain. As we introduced previously, the research of interfacial interaction of MREs has focused on the surface modification of CIPs. Hence, we would like to discuss the effect of vulcanization system on interfacial interaction of MREs based on NR in this work.

According to finite-element analysis, the best volume percent of CIPs for good MREs performance is about 30 vol%.²⁵ In this work, 30 vol% of CIPs was filled and sulfur and peroxide (dicumyl peroxide) were used as curing agents for preparing NR based MREs. Mechanical properties, crosslink density, and morphology were characterized to prove that the interfacial structure between CIPs and NR molecules were impacted by the vulcanization system. Finally, the modified dynamic thermomechanical analyzer (DMA) was used to examine the magneto-induced dynamic properties of MREs.

Experimental

Materials and Sample Preparation. Natural rubber (NR, RSS#1) was used as matrix of MREs. The magnetic particles, CIP, were provided by BASF with an approximate particle size of 3-5 μm and density of 7.8 g/cm³. The CIPs loading amount was fixed at 30 vol%.

The formula of NR with different vulcanization system was as follows:

(a) Sulfur system included sulfur, ZnO, stearic acid, and *N*-cyclohexyl-2-benzothiazolesulfenamide (CZ). The amounts of sulfur, ZnO, stearic acid, and CZ were 3.5, 6.0, 0.5, and 0.5 phr, respectively.

(b) Dicumyl peroxide (DCP) system had 2 phr of DCP mixed in the matrix.

The fabrication of MREs consisted of mixing, configuration, and curing. First, NR and CIPs were mixed using an open-roll mill at 55 °C for 10 min. Then, additives were mixed into NR and CIPs compound at 55 °C for 15 min. Finally, the compound was placed into a mold for pre-forming under an external magnetic field of 1300 mT and sufficient pressure, which was generated by the designed magnet-heat couple machine¹⁹ at 150 °C for 15 min. The compound was simultaneously cured at identical temperature and time.

The NR vulcanizates with sulfur and DCP will be referred to as NR-S and NR-DCP, respectively. MREs samples with sulfur and DCP will be referred to as MRE-S and MRE-DCP, respectively.

Characterization. Morphology and element analysis: The morphology of MREs was characterized by SEM (S-4300SE, HITACHI, Japan). The accelerating voltage was set to 15 kV. Before observation, the MREs were freeze-fractured using liquid nitrogen and coated with platinum to avoid surface charging. The energy dispersive spectroscopy (EDS) was used to analyze the surface element of CIPs in the MREs.

Crosslink Density: The crosslink density of elastomers was measured by the equilibrium swelling method.^{26,27} Samples were swollen in toluene at room temperature for 72 h and then removed from the solvent and the surface toluene was blotted off quickly using tissue paper. The samples were immediately weighed on an analytical balance and further dried in a vacuum oven for 36 h at 80 °C to remove all the solvent and reweighed. The volume fraction of AEM in the swollen gel, V_r , was calculated by the following eq. (1):

$$V_r = \frac{m_0 \times \phi \times (1 - \alpha) / \rho_r}{m_0 \times \phi \times (1 - \alpha) / \rho_r + (m_1 - m_2) / \rho_s} \quad (1)$$

where m_0 is the sample mass before swelling, m_1 and m_2 are sample masses before and after drying, ϕ is the mass fraction of rubber in the vulcanizate, α is the mass loss of the gum AEM vulcanizate during swelling, and ρ_r and ρ_s are the rubber and solvent density, respectively.

The elastically active network chain density, V_e , which was used to represent the whole crosslink density, was then calculated by the well-known Flory–Rehner eq. (2):

$$V_e = \frac{\ln(1 - V_r) + V_r + \chi V_r^2}{V_s(V_r^{1/3} - V_r/2)} \quad (2)$$

where V_r is the volume fraction of the polymer in the vulcanizate swollen to equilibrium and V_s is the solvent molar volume (107 cm³/mol for toluene). χ is the rubber–toluene interaction parameter and is taken as 0.57.²⁸

Mechanical Properties: The mechanical properties (tensile strength and elongation at break) were measured using a universal testing machine (DUT-500CM, Daekyung Engineering Co. Ltd, Korea) with a crosshead speed of 500 mm/min according to ASTM D412-06a. Five pieces of each sample were tested and the mean value was obtained.

Rubber Process Analyzer (RPA) Measurement: The dynamic storage modulus (G') of the NR and MREs based on NR were measured using an RPA (RPA2000, Alpha Technology, USA). The strain sweep was performed from 1° to 25° at 100 °C and 1 Hz. The frequency sweep was performed from

0.03 to 16.7 Hz at 100 °C and 1°.

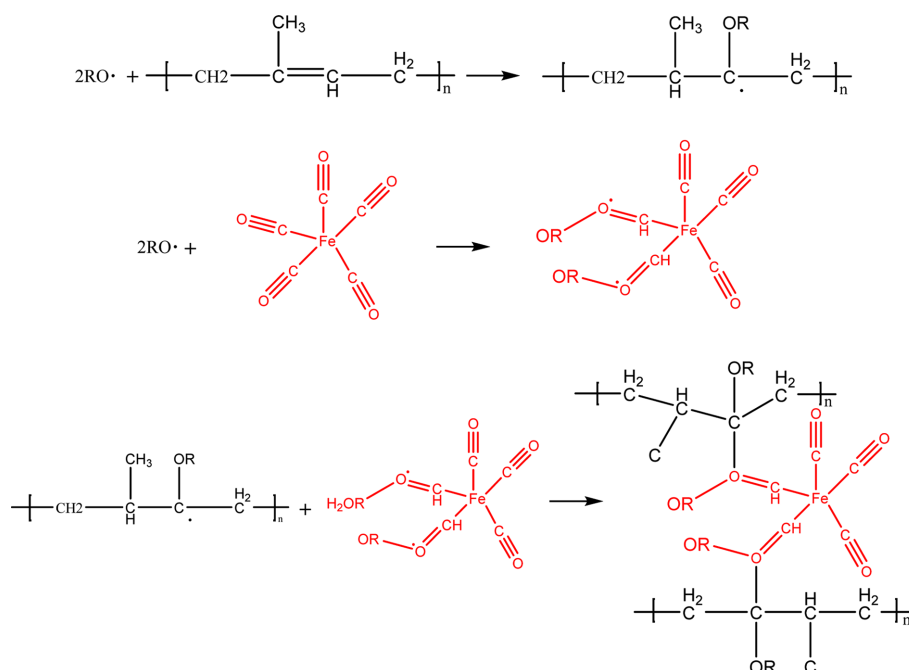
Dynamic Thermo-mechanical Analysis (DMA): DMA (Mettler Toledo Ltd, UK, model SDT861e) was performed to measure the dynamic properties, such as the storage modulus and loss modulus under different magnetic fields. This machine was designed by our group, but was assembled by Daekyung Engineering Co. Ltd, Korea. In this experiment, the CIP chain orientation was perpendicular to the direction of the shear stress force. The magnetic field was applied from 0 to 900 mT. The magnetic-induced properties were measured at room temperature from tests of the strain sweep and frequency sweep. Frequency sweeps were defined in the range of 1–15 Hz with a constant strain of 1%. Strain sweeps were further tested from 1–15% with a constant frequency of 1 Hz.

Results and Discussion

The Mechanism of Interfacial Interaction between CIPs and NR Molecules. Sulfur and DCP act as a crosslink agent in the vulcanization of NR. Sulfur cannot activate the carbonyl group on the surface of CIPs in the MRE based on NR. Therefore, interfacial interaction was not observed between CIPs and NR molecules. However, DCP is an oxidant, and is a common initiator in polymer synthesis. It decomposes and generates radicals at high temperature. The radicals not only make the NR molecules crosslink, but also activate the carbonyl bond on the surface of CIPs. Hence, interfacial interaction existed between NR molecules and CIPs, and the reaction mechanism is shown in Scheme 1.

Mechanical Properties and Crosslink Density. The mechanical properties of elastomers are crucial to engineering application. However, the mechanical properties of MREs decreased with the CIPs content because of the poor interfacial interaction.^{19,20} Table 1 and Figure 1 show the mechanical properties and crosslink density of NR vulcanizates and MREs with different curing agents, respectively. The tensile strength and elongation at break of NR-S were 22.5 MPa and 1170%, respectively. Those results were significantly higher than that of NR-DCP. The crosslink density of NR-S was 0.5×10^{-5} mol/cm³, which was larger than that of NR-DCP. Compared to DCP, sulfur was a better curing agent in NR matrix, and it resulted in better mechanical properties and larger crosslink density.

Same as previous work about MRE based on CR¹⁹ and EPDM,²⁰ the tensile strength of MRE-S decreased by the addition of 30 vol% of CIPs. However, the tensile strength of



Scheme 1. Reaction mechanism of carbonyl group on the CIPs surface and rubber molecules.

Table 1. Mechanical Properties of NR Vulcanizates and MREs with Different Curing Agents

	NR-DCP	MRE-DCP	NR-S	MRE-S
100% modulus (MPa)	0.83±0.03	0.92±0.06	1.02±0.11	0.98±0.06
300% modulus (MPa)	1.22±0.01	1.55±0.11	1.98±0.14	1.69±0.02
500% modulus (MPa)	2.76±0.19	3.19±0.23	3.91±0.41	3.30±0.08
Tensile strength (MPa)	14.52±1	16.04±1	22.50±3	20.18±1
Elongation at break (%)	808±10	647±5	1170±40	957±16

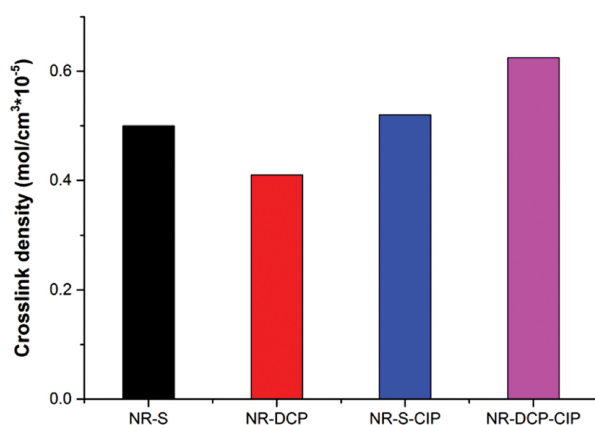


Figure 1. Crosslink density of NR vulcanizates and MRE with different cure agent.

MRE-DCP increased compared to NR-DCP. The elongation at break of MRE-S and MRE-DCP were both lower compared to the NR vulcanizates. The crosslink density of MRE-S was

similar to NR-S; however, the crosslink density of MRE-DCP was larger than that of NR-DCP. In fact, the crosslink density of MRE-DCP was the largest in all of samples. The results illustrated that there was not any interfacial interaction between NR molecules and CIPs under sulfur system, whereas the interfacial interaction existed between the NR molecules and CIPs under DCP curing system.

Dynamic Properties Measured by RPA. RPA is a dynamic mechanical rheological tester used to measure the dynamic properties of raw rubber, compound, and vulcanizates.²⁹ Figure 2 shows the storage modulus (G') response from strain (a) and frequency (b) sweep of NR vulcanizates and MRE with different curing system. The G' of all samples decreased with increasing strain intensity. Also, the G' of all samples slightly increased with increasing frequency. For the vulcanizates of NR, the G' of NR-S was higher than that of NR-DCP in the strain and frequency sweep. The G' of NR-

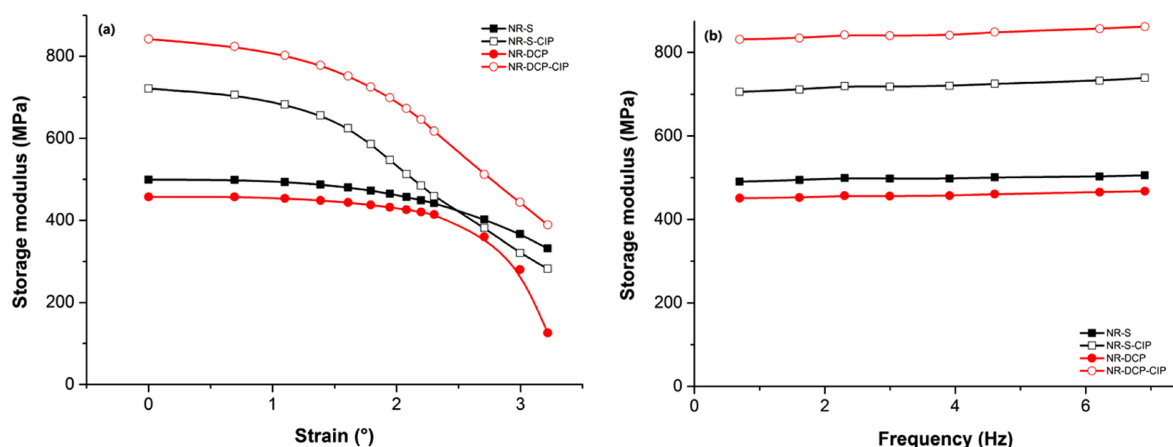


Figure 2. Storage modulus (G') of NR vulcanizates and MREs with different cure agent as function of strain and frequency.

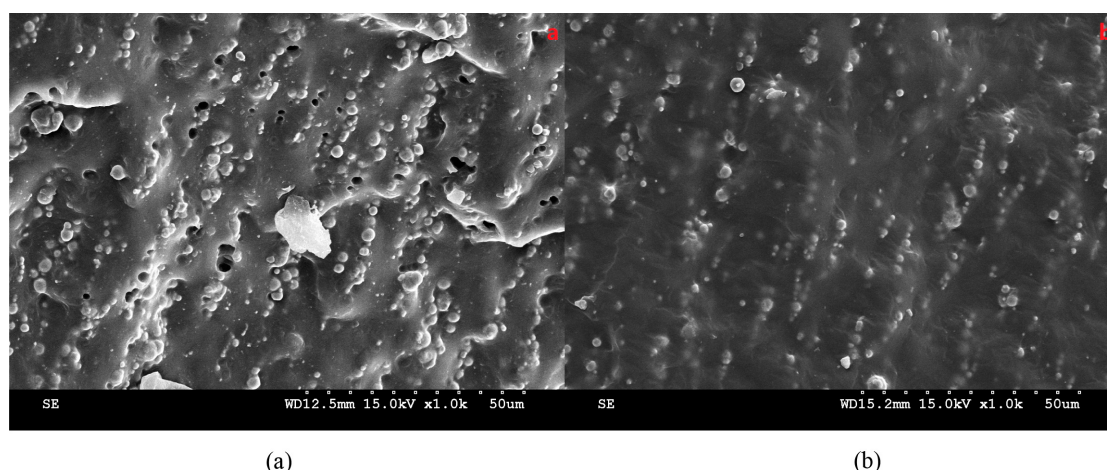


Figure 3. Morphology of MRE composites with different vulcanization system: (a) MRE-S; (b) MRE-DCP.

DCP sharply decreased at the high strain region. However, the G' of NR-S was higher than that of NR-DCP, and the decrease was not sharp as that of NR-DCP at the high strain region. The results illustrate that the crosslink structure of NR with sulfur system was more stable than the crosslink structure of NR with DCP system. The G' of MRE was higher than that of NR vulcanizates due to CIPs filled in the NR matrix. The MRE-DCP had the highest G' in the strain and frequency sweep. Except at the high strain sweep, the G' of MRE-S was higher than that of NR vulcanizates in the strain and frequency sweep. The G' of MRE-S was lower than that of NR-S at high strain, which was due to the lack of interfacial adhesion between CIPs and NR molecules. This resulted in the structure of MREs destroyed at the high strain. The results obtained using RPA, illustrated that there was interfacial interaction between CIPs and NR molecules, initiated by DCP, while the sulfur could not

initiate the reaction between CIPs and NR molecules. Hence, DCP enhanced the interfacial adhesion between CIPs and NR molecules, and resulted in higher crosslink density and storage modulus of MRE-DCP.

SEM and EDAX. Figure 3 compares the morphology of the MRE with different vulcanization system. The black holes in the Figure 3(a) were left by the CIPs that were removed during the freeze-fracture process. The surface of CIPs and the black holes are smooth, implying that there was not interfacial adhesion between CIPs and NR molecules in the sulfur system. Figure 3(b) was the CIPs dispersion in the NR with DCP system. Compared to the Figure 3(a), black holes were not observed and the surface of CIPs is coated by NR matrix in Figure 3(b). Figure 3 illustrated that interfacial interaction existed between CIPs and NR molecules with DCP curing system. Due to the good interfacial adhesion, the tensile strength

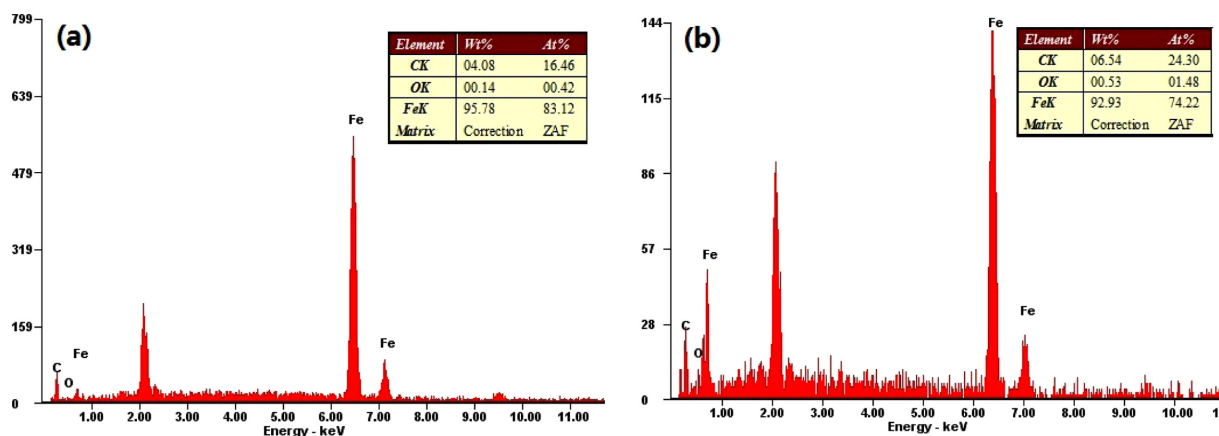


Figure 4. EDAX analysis of CIPs surface in the MRE matrix with different vulcanization system: (a) MRE-S; (b) MRE-DCP.

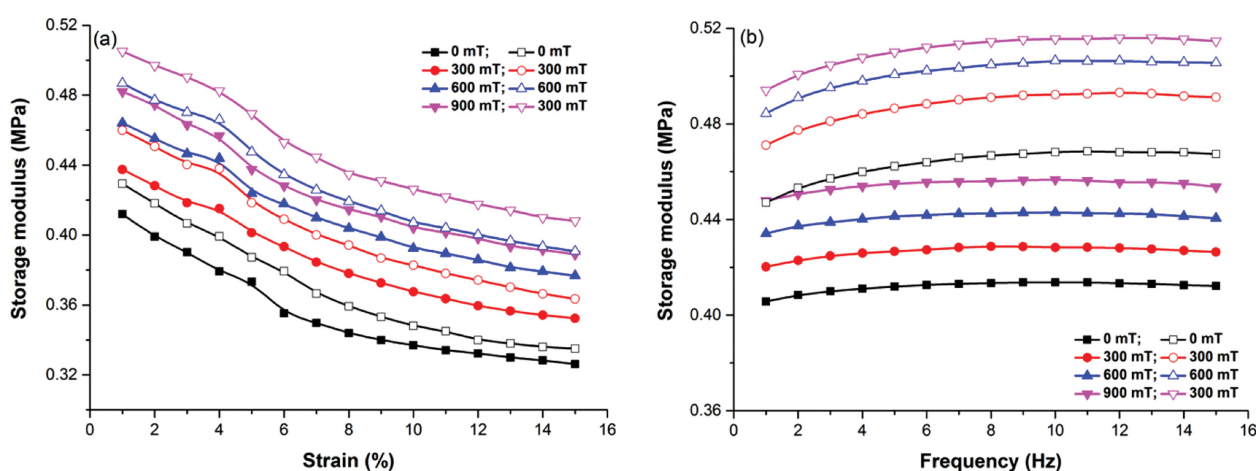


Figure 5. Storage modulus of MRE as function of strain (a); frequency (b) under various magnetic field intensity (closed symbol: MRE-S, open symbol: MRE-DCP).

of MRE-DCP was higher than that of NR-DCP. The mechanical properties of MRE-S became worse compared to NR-S. It resulted from no interfacial interaction between CIPs and NR molecules in the sulfur system.

Figure 4 shows the EDAX results of CIPs surface in the MRE matrix with different vulcanization system. The results showed that the CIPs surface in the MRE-S had higher of Fe ions content (95.78 wt%). The CIPs surface in the MRE-DCP have lower of Fe ions content (92.93 wt%), while the C content on the CIPs surface in the MRE-DCP was more than that in MRE-S. Additionally, the O ion content in the MRE-DCP was more than that in MRE-S. The results exhibited that the NR molecules adhered on the surface of CIPs in the MRE-DCP because DCP initiated the interfacial reaction between NR molecules and carbonyl group on CIPs surface.

DMA. Storage Modulus and $\Delta G'$: Figure 5 presents the

storage modulus (G') as function of strain (a) and frequency (b) exhibiting the elastic properties of the MRE-S (closed symbol) and MRE-DCP (open symbol). For the strain sweep, the measurements were tested by varying the applied strain from 1% to 15% with a constant frequency of 1 Hz. The G' decreased with increasing strain during strain sweep, which resulted from destroying the structure of MRE. With increasing magnetic field intensity, the G' of MRE was increased. Moreover, the G' of MRE-DCP was higher than that of MRE-S at the same intensity of magnetic field. For the frequency sweep, the measurements were tested by varying the applied frequency from 1 to 15 Hz with a constant strain of 1%. The G' slightly increased with increasing frequency during frequency sweep. The G' of MRE increased, with increasing the intensity of magnetic field. Compared to the G' under strain sweep, the G' of MRE-DCP was obviously higher than that of MRE-S, even

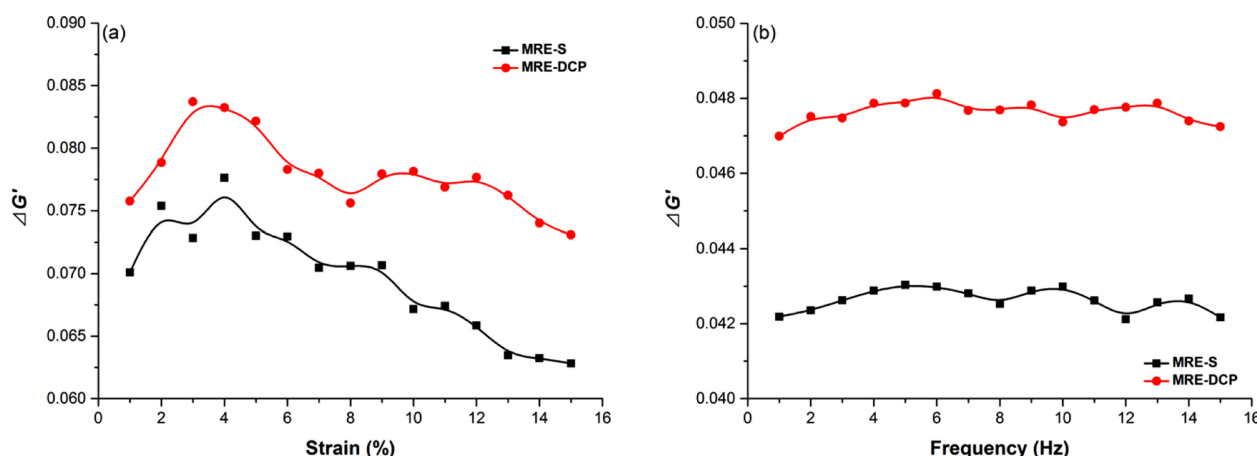


Figure 6. $\Delta G'$ of MRE as function of strain (a); frequency (b) under various magnetic field intensity.

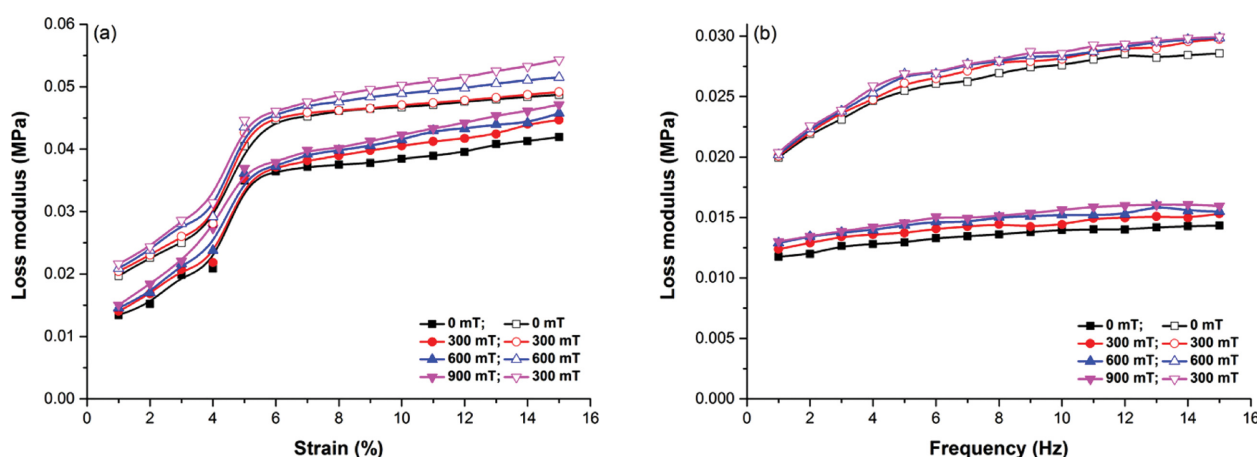


Figure 7. Loss modulus of MRE as function of strain (a); frequency (b) under various magnetic field intensity (closed symbol: MRE-S, open symbol: MRE-DCP).

though the G' of MRE-DCP at zero magnetic field was higher than that of MRE-S at 900 mT of magnetic field.

The $\Delta G'$ means the difference between G' at 900 mT of magnetic field (G'_{900}) and G' at zero-magnetic field (G'_0). This parameter presents the difference of G' under different magnetic fields. Hence, it could characterize the magnetic-induced efficiency of MRE. Figure 6 shows the absolute change in the storage modulus $\Delta G'$ ($\Delta G' = G'_{900} - G'_0$) for MRE with different curing agent system as a function of strain (a) and frequency (b). The results showed that $\Delta G'$ of MRE-DCP was higher than that of MRE-S, no matter the measurements tests under strain sweep or frequency sweep. The results showed that the DCP cured system improves the interfacial interaction between CIPs and rubber molecules, increases the G' of MRE, and also improved the magnetic-induced efficiency of MRE-DCP.

Loss Modulus: Loss modulus (G'') is a parameter to characterize the energy dissipated as heat in polymer materials. It represents the viscosity portion of the viscoelastic materials. Figure 7 shows the G'' of MRE as a function of strain (a) and frequency (b) sweep under various magnetic field intensity. The G'' increased with increasing strain over the entire range of strain. On the other hand, the G'' increased as the intensity of magnetic field increased. The G'' of MRE-DCP was higher than that of MRE-S over the entire range of strain. The G'' increased sharply when strain increased from 4% to 5%. This was caused by the network structure of MREs that were destroyed. In the frequency sweep, similar tendency was observed with strain sweep. The G'' increased with increasing the frequency and intensity of magnetic field. However, compared to strain sweep, the G'' of MRE-DCP was obviously higher than that of MRE-S at frequency sweep.

The results exhibited that the good interfacial adhesion led to higher viscous properties of MREs. Good interfacial compatibility between CIPs and rubber molecules resulted in good viscous properties and energy absorption.¹⁵

Conclusions

In this work, dicumyl peroxide (DCP) could initiate interfacial reaction between carbonyl group on the surface of CIPs and double bonds in NR molecules, hence, resulted in good interfacial interaction between CIPs and NR molecules. The results of SEM and EDAX demonstrated that the CIPs were coated by the NR molecules in MRE-DCP, and the elements of carbon and oxygen on the CIPs surface in the MRE-DCP were more than that of MRE-S. Due to the good interfacial adhesion, the MRE-DCP had higher crosslink density compared to MRE-S. The mechanical properties of MRE-DCP also increased compared to pure NR-DCP. According to the RPA results, the G' of MRE-DCP was higher than that of MRE-S because of the good interfacial adhesion in the MRE-DCP, even though the G' of NR-S was higher than that of NR-DCP. The G' and $\Delta G'$ of MRE-DCP measured by modified DMA under magnetic field was higher than that of MRE-S, no matter the strain sweep or frequency sweep. In addition, the loss modulus of MRE-DCP had similar tendencies with storage modulus of MREs and the G'' of MRE-DCP was higher than that of MRE-S. Overall, the MREs based on NR with DCP cured system showed good magneto-induced properties, which were caused by good interfacial compatibility between CIPs and rubber molecules.

Acknowledgement: The paper was supported the research grant of The University of Suwon in 2016.

References

1. J. D. Carlson and M. R. Jolly, *Mechatronics*, **10**, 555 (2000).
2. Y. D. Liu and H. J. Choi, *Mater. Res. Bull.*, **69**, 92 (2015).
3. H. L. Sun, P. Q. Zhang, X. L. Gong, and H. B. Chen, *J. Sound. Vib.*, **300**, 117 (2007).
4. M. H. Holdhusen and K. A. Cunefare, *J. Vib. Acoust.*, **129**, 577 (2007).
5. J. R. Watson, U.S. Patent 5609353 (1997).
6. S. H. Eem, H. J. Jung, and J. H. Koo, *IEEE T. Magn.*, **47**, 2901 (2011).
7. T. F. Tian, W. H. Li, and Y. M. Deng, *Smart Mater. Struct.*, **20**, 025022 (2011).
8. W. H. Li, K. Kostidis, X. Z. Zhang, and Y. Zhou, in *IEEE/ASME International Conference on Advanced Intelligent Mechatronics (AIM)*, p 233 (2009).
9. M. Farshad and M. L. Roux, *Polym. Test.*, **23**, 855 (2004).
10. I. Bica, *J. Ind. Eng. Chem.*, **15**, 773 (2009).
11. L. Chen, X. L. Gong, and W. H. Li, *Polym. Test.*, **27**, 340 (2008).
12. K. H. Chung, U. C. Jeong, and J. E. Oh, *Polym. Eng. Sci.*, **55**, 2669 (2015).
13. L. Ge, X. L. Gong, Y. C. Fan, and S. H. Xuan, *Smart Mater. Struct.*, **22**, 115029 (2013).
14. H. S. Jung, S. H. Kwon, H. J. Choi, J. H. Jung, and Y. G. Kim, *Compos. Struct.*, **136**, 106 (2016).
15. J. S. An, S. H. Kwon, H. J. Choi, J. H. Jung, and Y. G. Kim, *Compos. Struct.*, **160**, 1020 (2017).
16. K. L. Pickering, S. R. Khimi, and S. Ilanko, *Composites Part A*, **68**, 377 (2015).
17. X. C. Guan, X. F. Dong, and J. P. Ou, *J. Magn. Magn. Mater.*, **320**, 158 (2008).
18. T. Mitsumata, S. Ohori, N. Chiba, and M. Kawai, *Soft Matter*, **42**, 10108 (2013).
19. Y. H. Wang, X. R. Zhang, J. E. Oh, and K. H. Chung, *Smart Mater. Struct.*, **24**, 095006 (2015).
20. Y. H. Wang, X. R. Zhang, K. H. Chung, C. C. Liu, S. B. Choi, and H. J. Choi, *Smart Mater. Struct.*, **25**, 115028 (2016).
21. Y. C. Fan, X. L. Gong, S. H. Xuan, W. Zhang, J. Zheng, and W. Q. Jiang, *Smart Mater. Struct.*, **20**, 035007 (2011).
22. J. Kruzalak, R. Sykora, and I. Hudec, *Rubber Chem. Technol.*, **90**, 60 (2017).
23. Y. Ikeda, Y. Yasuda, K. Hijikata, M. Tosaka, and S. Kohjiya, *Macromolecules*, **41**, 5876 (2008).
24. T. M. Gao, R. H. Xie, L. H. Zhang, P. W. Li, H. X. Gui, M. F. Huang, and K. H. Chung, *Polym. Korea*, **40**, 446 (2016).
25. L. C. Davis, *J. Appl. Phys.*, **85**, 3348 (1999).
26. P. J. Flory and J. Rehner, *J. Chem. Phys.*, **11**, 521 (1943).
27. P. J. Flory, *J. Chem. Phys.*, **18**, 108 (1950).
28. B. C. Guo, F. Chen, Y. D. Lei, X. L. Liu, J. J. Wan, and D. M. Jia, *Appl. Surf. Sci.*, **255**, 7329 (2009).
29. P. Y. Wang, H. L. Qian, C. L. Yang, and Y. Chen, *J. Appl. Polym. Sci.*, **100**, 1277 (2006).